Electronic Supplementary Material (ESI) for Journal of Materials Chemistry A.

Supplementary Information

Interwoven MoO_3@CNT Scaffold Interlayer for High-Performance Lithium-Sulfur Batteries

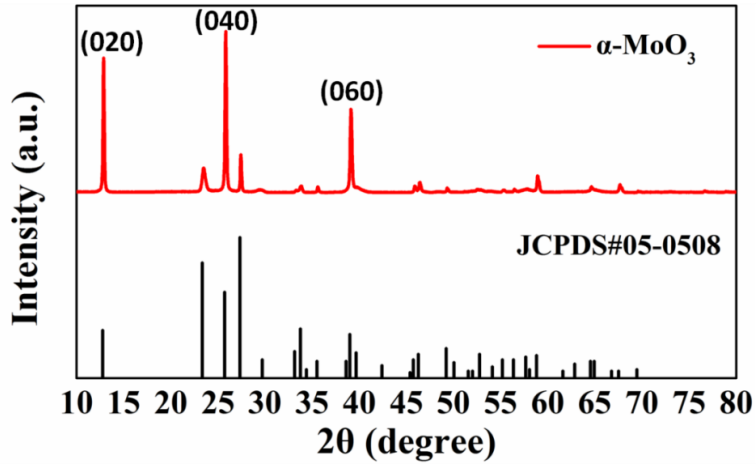

Figure S1. XRD pattern of MoO_3 nanorods.

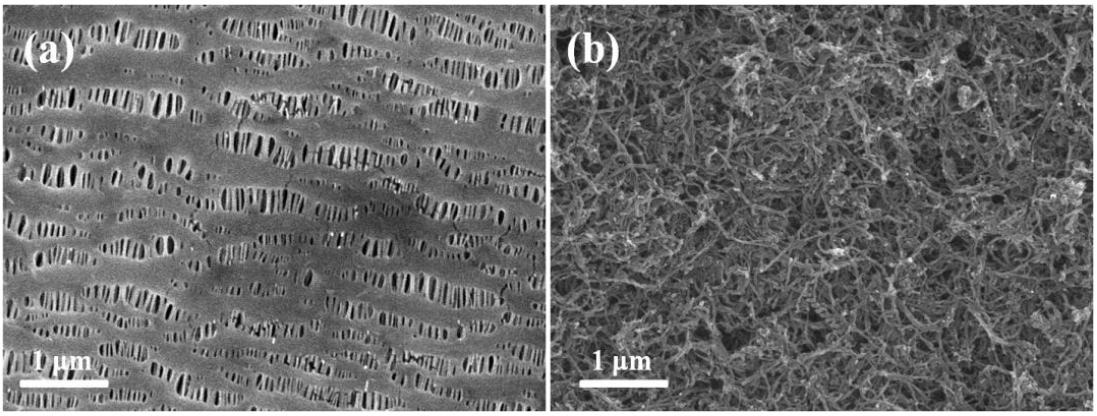

Figure S2. SEM images of original PP separator (a) and CNT decorated separator (b).

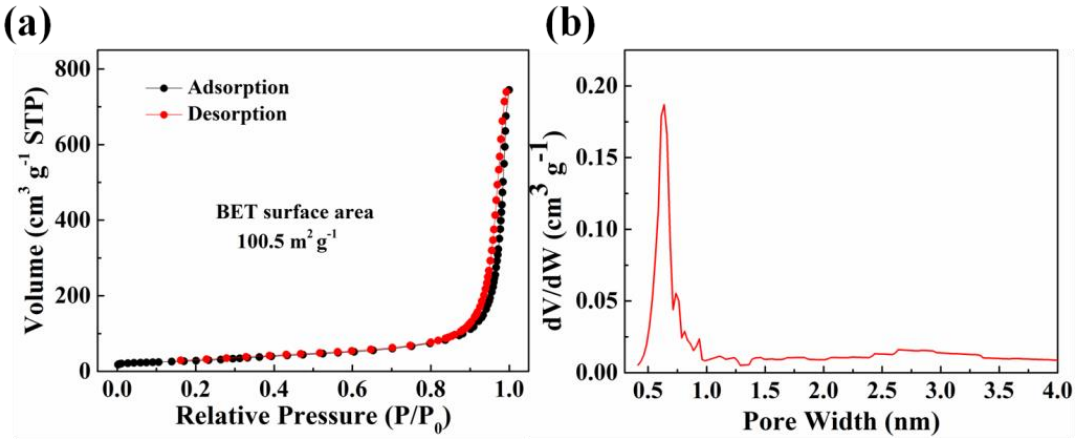

Figure S3. N_2 adsorption-desorption isotherms (a) and pore size distribution (b) of CNT powders.

Table S1 Simulated resistance parameters of cells with different separators.

Battery Type / Cycle Number	MoO_3@CNT-PP		CNT-PP		PP		
	$R_b(\Omega)$	$R_{ct}(\Omega)$	$R_b(\Omega)$	$R_{ct}(\Omega)$	$R_b(\Omega)$	$R_{sei}(\Omega)$	$R_{ct}(\Omega)$
Fresh Cell	4.66	26.65	4.99	23.92	3.56	-	34.67
After 100 Cycles	3.77	4.31	3.48	6.91	5.75	20.84	11.11

Based on the calculation method of lithium-ion diffusion coefficient, the equations are shown as below:[1]

$$Z' = R_D + R_L + \sigma\omega^{-1/2} \quad (1)$$

$$D_{Li} = \frac{R^2T^2}{2A^2n^4F^4C^2\sigma^2} \quad (2)$$

where D_{Li} represents the diffusion coefficient of the lithium ion, R is the gas constant, T the absolute temperature, A the surface area of electrode, n the number of electrons per molecule during oxidization, F the Faraday constant, C the concentration of lithium ion, and σ the Warburg factor, σ relates to Z' and its value can be obtained from the slope of the lines between Z' and $\omega^{-1/2}$.

The low frequency part of the Nyquist plot represents the Warburg impendence related to the lithium ion diffusion.[2] As the electrochemical model of the cell with PP separator is different with the others, we choose low frequency part of EIS results of

the cells with MoO_3@CNT-PP and CNT-PP after cycling. The relation between Z' and $\omega^{-1/2}$ is shown in Fig. R6. After fitting, the cell with MoO_3@CNT-PP possess a much lower σ value of 21.72 than the cell with CNT-PP with σ value of 140.32. Since it is hard to determine the lithium-ion concentration with the phase change in the sulfur cathode, based on the equation (2), it can be concluded qualitatively that the ion diffusion of the cell with MoO_3@CNT-PP is quite faster than the cell with CNT-PP.

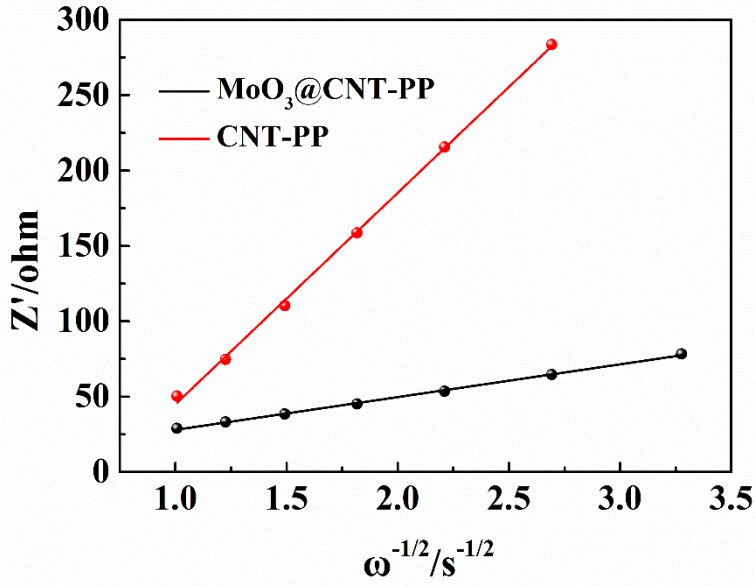

Fig. S4 Real parts of the complex impedance of cells with MoO_3@CNT-PP and CNT-PP versus $\omega^{-1/2}$ after cycling.

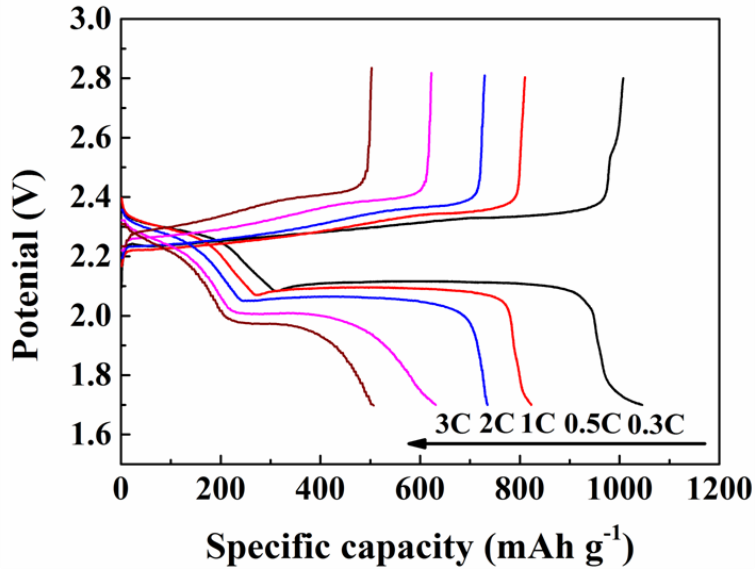

Figure S5. Discharge-charge curves of Li-S batteries with CNT-PP separator.

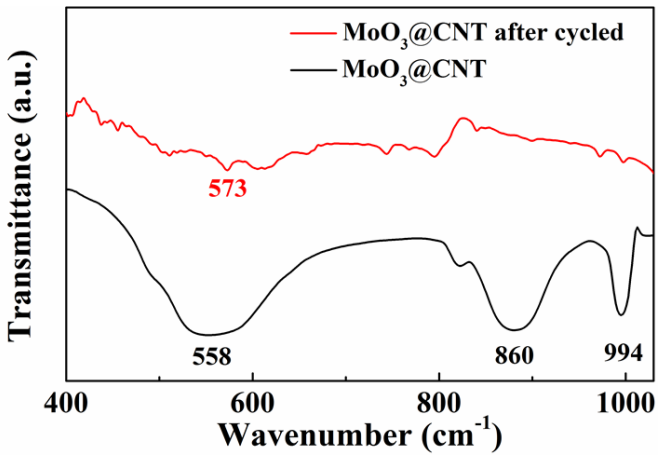

Figure. S6 FT-IR spectra of original MoO_3@CNT and cycled one in Li-S battery.

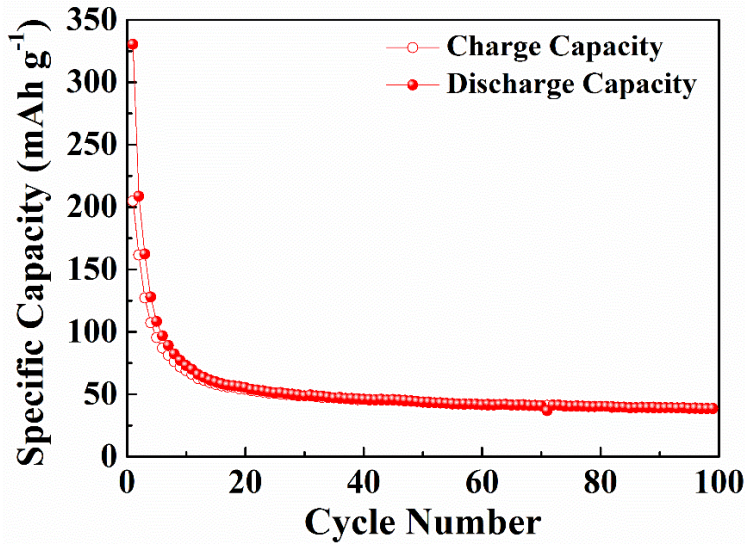

Figure S7 Cycling performance of the cell using MoO_3@CNT as the only active material.

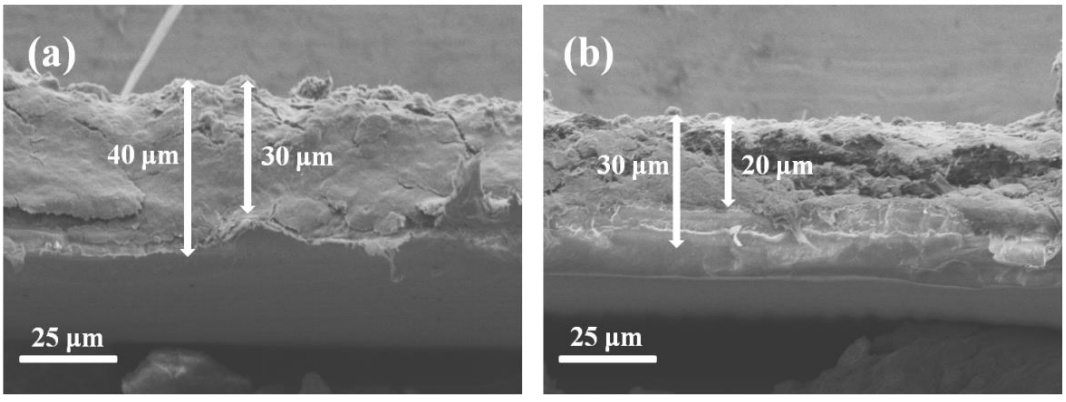

Figure S8. Cross-sectional SEM images of modified separators with CNT (a) and MoO_3@CNT (b) as the coating layers.

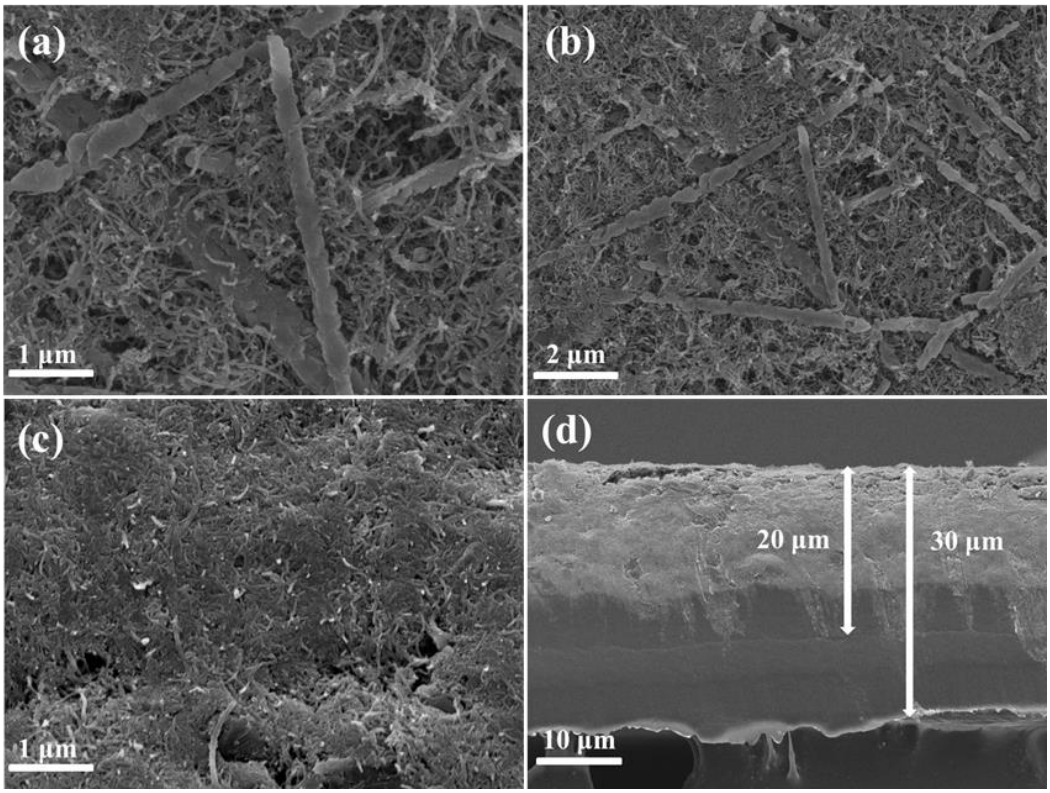

Figure. S9 SEM images of MoO_3@CNT-PP separator after cycling: surface morphology (a, b) and cross-sectional structure (c, d).

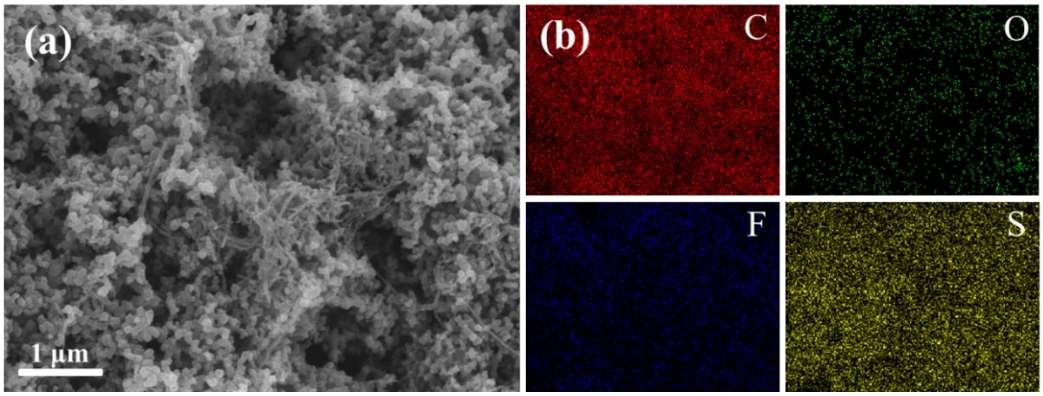

Figure. S10 SEM image (a) and EDS mapping images (b) of the sulfur cathode after cycling.

Reference

1. B. Li, C. Han, Y.-B. He, C. Yang, H. Du, Q.-H. Yang and F. Kang, *Energy & Environmental Science*, 2012, **5**, 9595.